

Supersonic Wind Tunnel Simulation of Propulsive Jets

R.A. White*

University of Illinois at Urbana-Champaign, Urbana, Illinois
and

J. Agrell† and S.-E. Nyberg‡

Aeronautical Research Institute of Sweden, Bromma, Sweden

This paper describes improvements in a modeling methodology for congruent plumes produced from nonideal nozzle flows and a series of verification tests including complex afterbody and wake flows caused by angle of attack and afterbody-mounted control fins at incidence. The results show that the modeling methodology gives good agreement for the base pressure and separation location for stagnation pressure ratios of $\pm 25\%$ from the design condition, for angles of attack as high as ± 20 deg, and with the effects of control fins deflected ± 10 deg in conjunction with angle of attack of ± 6 deg. A small but systematic difference between the prototype and model results is evident and a possible explanation is offered.

Nomenclature

D	= forebody diameter, m
L	= boattail length, m
M_E	= freestream Mach number
M_F	= surface Mach number
M_L	= lip Mach number§
P_b, P_B	= base pressure, Pa
P_E, P_e	= freestream static pressure, Pa
P_L	= lip pressure, Pa
P_{OE}	= stagnation pressure, Pa
P_{OI}	= nozzle stagnation pressure, Pa
R_C	= initial surface curvature, m
R_L	= exit or lip radius, m
S	= separation distance measured from end of boattail, m
T_{OI}	= nozzle stagnation temperature, °C
U	= axial velocity in the boundary layer
U_E	= freestream velocity
α	= angle of attack, deg; see Fig. 5
β	= boattail angle, deg; see Fig. 1
γ	= ratio of specific heats
δ	= control deflection angle, deg; see Fig. 5
$\Delta(P_B/P_E)_\alpha$	= effect of angle of attack on base pressure, $(P_B/P_E)_\alpha - (P_B/P_E)_{\alpha=0}$
$\Delta(P_B/P_E)_\delta$	= effect of controls on base pressure, $(P_B/P_E)_{\text{with controls}} - (P_B/P_E)_{\text{without controls}}$
θ_F	= initial surface slope, deg
θ_L	= conical divergence angle, deg
θ_L	= circumferential angle, deg; see Fig. 5
ω_F	= Prandtl-Meyer angle corresponding to M_F , deg
ω_L	= Prandtl-Meyer angle corresponding to M_L , deg

Subscripts

A	= air
F	= Freon
M	= model
P	= prototype

Presented as Paper 84-0230 at the AIAA 22nd Aerospace Sciences Meeting, Reno, Nev., Jan. 9-12, 1984; received Feb. 2, 1984; revision received July 12, 1984. Copyright © American Institute of Aeronautics and Astronautics, Inc., 1984. All rights reserved.

*Professor of Mechanical Engineering.

†Research Scientist.

‡Consultant; formerly Deputy Head, Aerodynamics Department.

§Conical source flow assumed, otherwise nozzle geometry and lip conditions are specified in greater detail, see Ref. 15.

Introduction

UNDERSTANDING the interaction of rocket or jet plumes with the external flowfield and surrounding launch equipment or adjacent surfaces is crucial to the prediction of total system performance.¹ Such interactions determine the near-wake base pressure and temperatures, the flow over portions of the vehicle surface in the case of upstream external flow separation, the wake flowfield at angle of attack, afterbody-mounted control surface effectiveness, and launch equipment performance. The plume-slipstream interference flowfield affects aerodynamic performance by introducing drag penalties through lower than ambient base pressure or leads, as the ratio of jet stagnation-to-ambient pressure increases as for highly accelerated vehicles, to plume-induced separation.² In extreme conditions, such separation can lead to loss of stability and/or degradation of control effectiveness.³

The understanding of plume-induced separation is, therefore, a vital factor in missile design. The interdependence of theory, design, and modeling to prototype development and eventually to operational vehicles is clearly essential. Indeed, modeling, particularly with respect to wind tunnel testing, spans the entire development lifetime of a missile design.

The generation of rocket or jet plumes in wind tunnel investigations must, consequently, account for all or part of the factors affecting the induced flowfield (see Fig. 1), including plume shape, plume deflection, mass entrainment along the shear layer, wake closure (impingement), viscous and dynamic effects, temperature, influence of specific heat ratio and molecular weight, and possibly energy release through chemical reactions. The difficulty in attempting to simulate all of these parameters simultaneously is well known.⁴ Since all parameters cannot, in general, be simulated simultaneously in a wind tunnel, it becomes essential to determine the importance of the individual factors discussed above. This information has, in general, been lacking although recent simulation studies⁵ have contributed strongly to this area of knowledge. The importance of a plume modeling methodology is obvious due to the fact that strictly empirical correlations have been utilized for such important applications as the Space Shuttle.

The plume simulation question is consequently of particular significance, since the hope of accurately computing (using CFD) complex flowfields of the type shown in Fig. 2, or determining practical empirical correlating parameters for such flows, is remote at this time. Consequently, the design of rocket-propelled missiles will rely on wind tunnel testing and proper plume simulation for the foreseeable future.

For a known pressure distribution over the prototype afterbody due to the nonseparated slipstream, one can estimate the pressure rise due to separation. The resulting plateau pressure determines the jet surface Mach number $M_{F,P}$ so that the prototype conditions are all given, and the model nozzle exit con-

ditions $M_{L,M}$, $\theta_{L,M}$, as well as the model jet surface Mach number $M_{F,M}$, are determined.¹⁰

In the vicinity of this design point, only the more stringent condition of plume slope matching is retained. This can be expressed in the form

$$\theta_{F,M} = \theta_{F,P} \quad (2)$$

and

$$\omega_{F,P} = \theta_{L,M} - \theta_{L,P} + \omega_{L,P} - \omega_{L,M} - \omega_{F,M} \quad (3)$$

Experimental Equipment

Simulation Test Facility

The wind tunnel used in this investigation of plume simulation by compressed air and Freon-22 is the FFA's Tunnel S5.¹⁵ It is of an intermittent suck-down type and has two-dimensional solid nozzle blocks for supersonic speeds and a test section 0.45×0.57 m. Tunnel stagnation pressure and temperature are approximately equal to atmospheric conditions.

Compressed dry air for plume simulation is available from high-pressure storage facilities,¹⁵ which allows the storage of 50 m^3 of air at a pressure of 25 MPa. The temperature can be selected in the range -20 to $+300^\circ\text{C}$ and the maximum flow-rate is 2.7 kg/s .

A hot-gas facility, primarily intended for various types of heated Freon, is available for plume simulation. Freon-22 has been chosen for all tests to date,⁵ as well as the present study. The ratio of specific heats, γ at the nozzle exit and for plume expansion conditions, is in the range of 1.16 to 1.18, which is appropriate for simulation of combustion-type jet products.

Selection of Design Condition and Model Geometries

Since the specific heat ratio for Freon-22 is appropriate for simulation of combustion-type jet products, it is appropriate for the prototype gas for simulation in wind tunnels. The geometry of the prototype nozzle was chosen to be as realistic as possible, e.g., to have a shape similar to a typical rocket nozzle (see Fig. 3a, $M_{L,P} = 2.60$, $R_{L,P} = 15^\circ$ deg and $P_L/P_E|_P = 3.48$). The calculated data^{5,10} of the model air nozzles are $M_{L,M} = 1.41$, $R_{L,M} = 3.07^\circ$ deg, and $P_L/P_E|_M = 6.03$ for separation flow modeling; and $M_{L,M} = 2.03$, $R_{L,M} = 10.47^\circ$ deg, and $P_L/P_E|_M = 5.07$ for base pressure modeling.

Wind Tunnel Model

The basic model shown in Fig. 4 is built up of a 14° half-angle nose cone, a cylindrical centerbody of 50 mm diameter, and a set of interchangeable afterbodies and propulsive nozzles. The overall length is 9.5 diameters. The model is supported just behind the conical nose by a strut with 40° deg sweep back which also acts as the inlet channel for the gas jet. The rear part of the centerbody, the boattail, and the base region are all instrumented with pressure taps. A set of four stabilizing or control fins can be attached to the afterbody as shown in Fig. 5. In this test, the controls were positioned circumferentially at $\phi = \pm 45$ and $\pm 135^\circ$ deg. The four controls has a bicircular arc airfoil of 8% thickness, a span of 1.11 diameter, a root chord of 1.0 diameter, and a tip chord of 0.55 diameter. The controls could be set at deflection angles of $\delta = 0$ and $\pm 10^\circ$ deg.

Transition trips were applied on the conical nose of the model, 85 mm from the apex and on control surfaces 4 mm from the leading edge.

Plume Modeling Experiments

Test Conditions

The tests were carried out in the FFA's S5 wind tunnel¹⁵ at a freestream Mach number $M_E = 2.0$ and a corresponding Reynolds number 6×10^6 based on the model length. The nozzles were tested at the design stagnation pressure and at pressures 25% below and above this value. The nominal propulsive jet stagnation conditions used are shown in Table 1.

Table 1 Propulsive jet stagnation conditions

Propellant	Nozzle, M_L	Stagnation pressure, MPa			Stagnation temperature, $^\circ\text{C}$
Freon	2.6	0.76	1.00	1.25	104-150
Air	1.41	0.19	0.25	0.30	-20-20
Air	2.03	0.40	0.53	0.66	-20-20

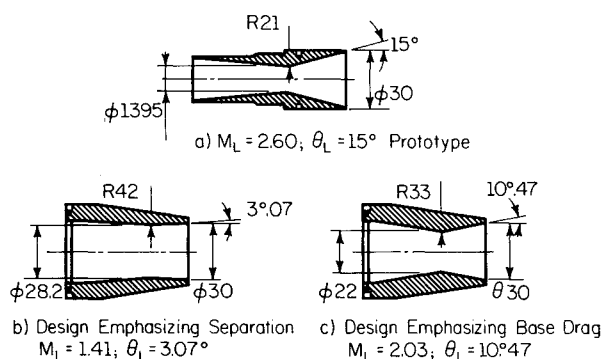


Fig. 3 Prototype nozzle with $\gamma = 1.16$ and two model nozzles (air, $\gamma = 1.40$) emphasizing different operating conditions.

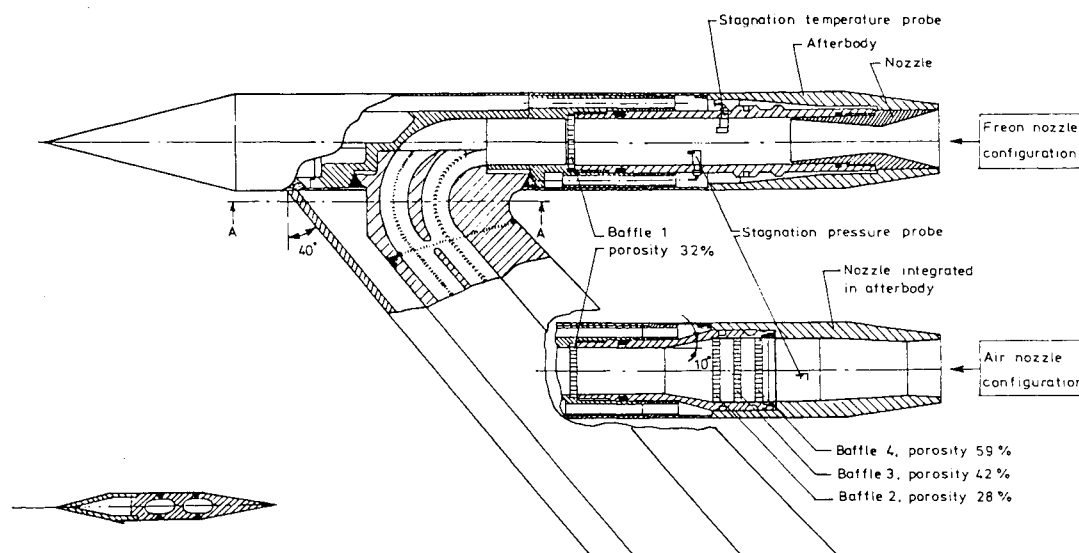


Fig. 4 Model and nozzle system.

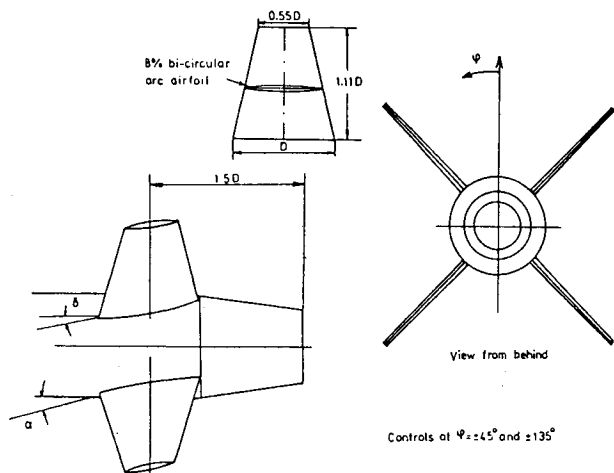


Fig. 5 Control dimensions and definition of control deflection angles.

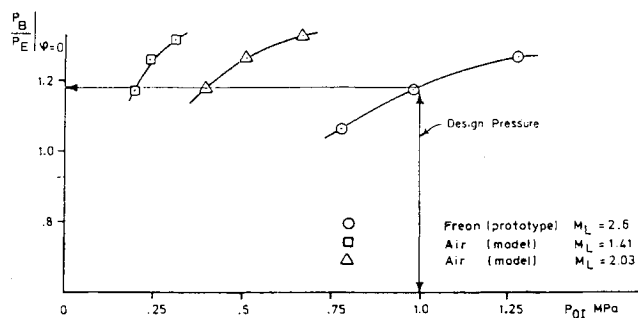


Fig. 6 Base pressure ratio for Freon (prototype) and air (model) vs nozzle stagnation pressure.

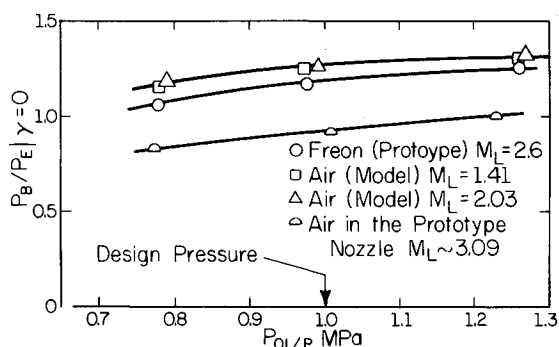


Fig. 7 Base pressure ratio for Freon (prototype) and air (model) vs nozzle prototype stagnation pressure.

The presentation of angle of attack and control fin effects is limited herein to the design jet stagnation pressure. The off-design pressure results have been published in Ref. 16.

Zero-Angle-of-Attack Results

Base pressure ratios, P_B/P_E , measured for the Freon (prototype) and air (model) nozzles vs the jet stagnation pressure P_{01} , as measured in the settling chamber of the nozzle, are shown in Fig. 6. The same base pressure ratios with the air (model) nozzle results transformed into the Freon (prototype) plane are plotted vs the prototype stagnation pressure in Fig. 7. The two air (model) nozzle results agree very well with each other, and the correlation with the Freon (prototype) nozzle results is quite good. Also shown for comparison are the results of using cold air in the prototype nozzle (no modeling). The poor agreement with the Freon results is obvious. It is believed, however, that the discrepancy between

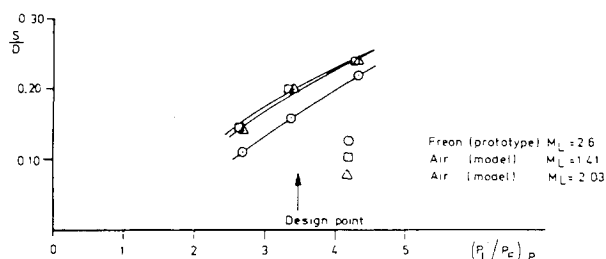


Fig. 8 Separation location vs lip pressure for Freon (prototype) and air (model) nozzles.

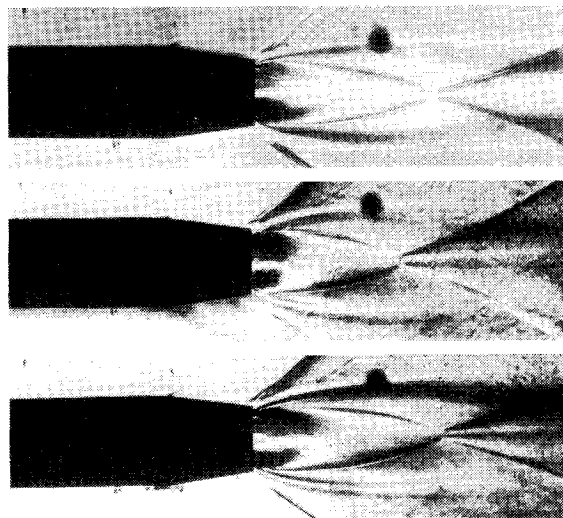


Fig. 9 Schlieren photographs from tests at design conditions ($\alpha = 0$; $P_{01} = 1.0$ MPa).

the prototype and the model results is significant despite being fairly small.

A possible explanation for the discrepancy lies in the fact that the calculation of the air (model) nozzle neglected viscous effects along the wake and during the impingement process. The possibility of modifying the recompression model to account for differences in mixing is being studied.

The afterbody flow separation location as determined from longitudinal pressure distributions and from schlieren photographs is shown vs prototype lip pressure ratio in Fig. 8 for the Freon (prototype) and air (model) nozzles. Again the air results agree very well, but a minor systematic discrepancy between Freon (prototype) and air (model) seems to be established.

Schlieren pictures of the flow for the three nozzles at the design stagnation pressure are presented in Fig. 9 together with a plot overlay of some of the significant features in the pictures. In this scale, no differences in plume shape have been observed, but minor differences in the location of the separation shock are detected and appreciable differences in the shape of the inner (barrel) shock are noticed. The latter is to be expected due to the difference in nozzle flowfield Mach number.

Effects of Angle of Attack

Although the modeled nozzles have been calculated for axisymmetric flow, tests have been made at low angles of attack

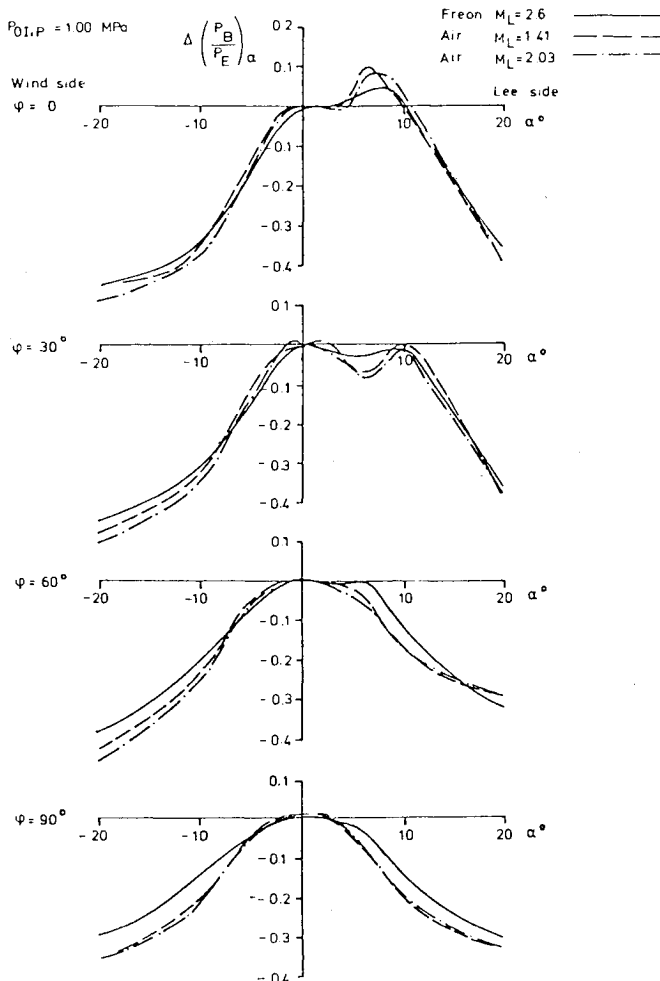


Fig. 10 Effect of angle of attack on base pressure ratio $\Delta(P_B/P_E)_\alpha = (P_B/P_E)_\alpha - (P_B/P_E)_{\alpha=0}$ vs angle of attack α at stagnation pressure $P_{0I,P} = 1.0$ MPa = design pressure.

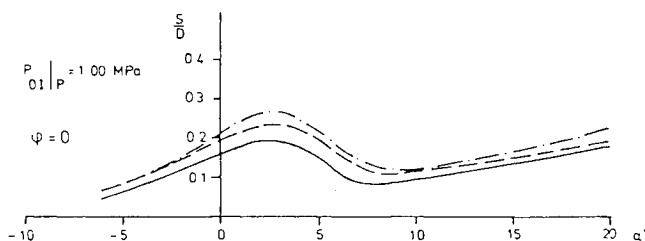


Fig. 11 Separation location S/D at $\phi = 0$ vs angle of attack α for Freon (prototype) and air (model) nozzles at stagnation pressures $P_{0I,P} = 0.76, 1.0$, and 1.25 MPa.

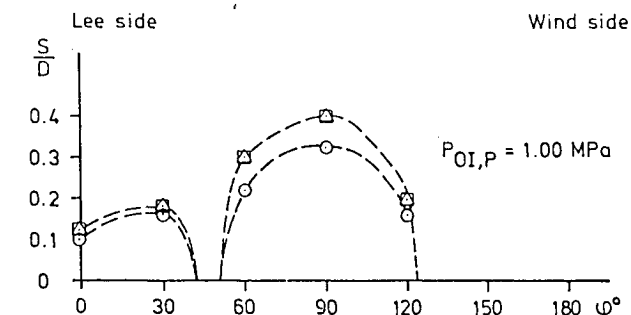


Fig. 12 Separation location S/D at $\alpha = 10$ deg from pressure measurements vs circumferential angle ϕ for Freon (prototype) and air (model) nozzles at stagnation pressures $P_{0I,P} = 0.76, 1.0$ and 1.25 MPa. The dotted lines show the separation line obtained from oil flow pictures as in Fig. 13.

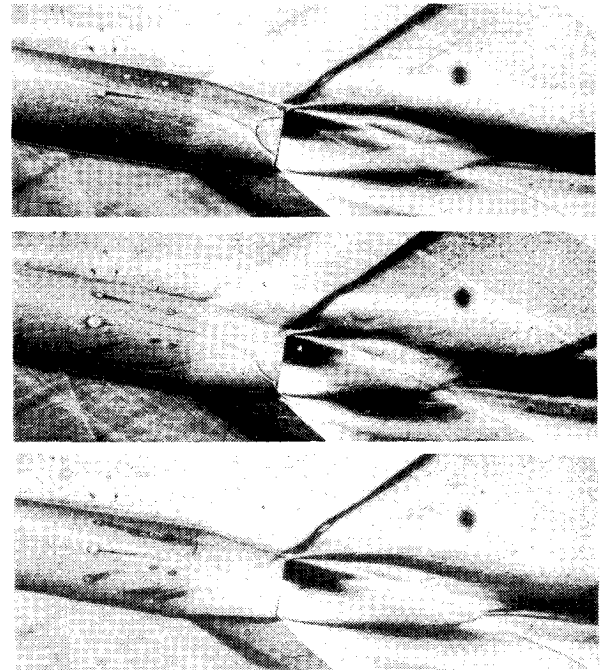


Fig. 13 Oil flow and schlieren photograph at $\alpha = -10$ deg and $P_{0I,P} = 1.0$ MPa for Freon (prototype) and air (model) nozzles.

($-6 \text{ deg} \leq \alpha \leq +6 \text{ deg}$)⁶ and at high angles of attack ($-20 \text{ deg} \leq \alpha \leq +20 \text{ deg}$)⁷⁻⁹ to examine the limits of the modeling procedure. To facilitate the evaluation of the simulation of the angle-of-attack effects on the base pressure, the difference $\Delta(P_B/P_E)_\alpha = (P_B/P_E)_\alpha - (P_B/P_E)_{\alpha=0}$ is shown as a function of angle of attack in Fig. 10 for the three nozzles. It can be seen that the angle-of-attack effect of the Freon (prototype) nozzle is simulated quite well. It is, however, also observed that the agreement between the two air nozzle results is generally very good and that the discrepancy between the Freon and air results has the same character as at zero angle of attack. Therefore, in most cases, there is a slightly stronger angle-of-attack effect on the base pressure with the air nozzles than there is with the Freon nozzle.

The separation location S/D at the circumferential angle $\delta = 0$ is shown in Fig. 11 vs angle of attack. The simulation is quite good, except at low positive angles of attack or on the lee side where the vortex flow starts to build up. The two air nozzle results agree very well, and the discrepancy between the Freon and the air results are, as could be expected, of the same character as the base pressure results.

Shown in Fig. 12 is a sample of the circumferential variation of the separation location at angle of attack $\alpha = 10$ deg as obtained from pressure measurement. Oil flow and schlieren pictures for the same angle of attack and pressure ratio are presented in Fig. 13. The separation lines shown in Fig. 12 have been drawn using the detailed information from oil flow pictures. It is obvious from these figures that the circumferential variation of the separation location is simulated quite well at this angle of attack, but the correlation is better between the air results than it is between Freon and air. In general, the results confirm that the basic validity of the Korst modeling methodology is satisfactory within the angle-of-attack range investigated ($-20 \text{ deg} \leq \alpha \leq 20 \text{ deg}$).

Effect of Control Fins

Wind tunnel tests have been carried out to investigate effects of the afterbody being exposed to the complex external flowfield generated by aft-mounted controls in combination with angle of attack. The angle-of-attack range was $-6 \text{ deg} \leq \alpha \leq +6 \text{ deg}$ and the controls were set at $\delta = 0$ and ± 10 deg.

To isolate the effects of controls on the base pressure ratio more clearly, the difference between the results with and

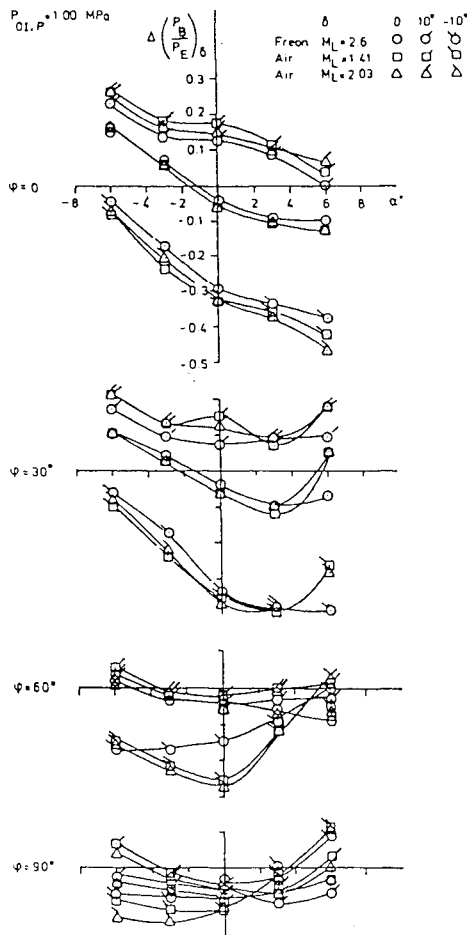


Fig. 14 Effect of controls on base pressure ratio $\Delta(P_B/P_E)_\delta = (P_B/P_E)_{\text{with controls}} - (P_B/P_E)_{\text{without controls}}$ vs angle of attack α at stagnation pressure $P_{01,P} = 1.0$ MPa.

without controls have been calculated for comparison, and results for all three nozzles have been plotted together in Fig. 14 vs angle of attack. The results are at the design jet stagnation pressure for the circumferential angles investigated. Selected schlieren pictures are presented in Fig. 2.

After analysis of the test results, it was concluded that the effect of the fins on base pressure obtained with the Freon (prototype) nozzle was, in general, satisfactorily simulated by the air (model) nozzles. The few local exceptions seem to occur in areas where interaction between the control wake and the separated base region might be very sensitive to one parameter, e.g., the jet stagnation pressure. Apart from these few points, the modeling seems to be valid even for severe combinations of control angles, angle of attack, and off-design jet stagnation pressure. It is noted, however, that the effect of controls on base pressure ratio obtained with the air (model) nozzles is often somewhat larger than the effect with the Freon (prototype) nozzle.

Conclusions

A program has been undertaken to examine the limits of the plume modeling methodology proposed by Korst. This paper covers wind tunnel tests carried out at Mach number $M_E = 2.0$ with one Freon (prototype) nozzle and two air (model) nozzles. An analysis of the experimental results obtained allows the following conclusions:

- 1) The basic validity of the Korst modeling methodology, established in an earlier study, was confirmed. The methodology correlates both base pressure and flow separation in the vicinity of the base of the prototype and modeled nozzles.
- 2) Although the total scatter in the correlation between Freon (prototype) and air (model) nozzles is the same as in

earlier tests,⁵ in the current test results there are indications of a minor systematic discrepancy between the Freon and air results. A possible explanation is suggested.

3) The modeled results are good even if the jet stagnation pressure deviates $\pm 25\%$ from the design pressure.¹⁶

4) The modeling scheme is satisfactory even at high angles of attack, $\alpha = \pm 20$ deg.

5) The effects of aft-mounted control fins are simulated satisfactorily. This includes cases where the controls are deflected ($\delta = \pm 10$ deg) in combination with angle of attack ($-6 \text{ deg} \leq \alpha \leq +6 \text{ deg}$).

Acknowledgments

This research program is supported jointly by the European Research Office, U.S. Army, Contract DAJA37-81-C-1213, The Aeronautical Research Institute of Sweden (FFA), and the U.S. Army Research Office under Grant DAAG-29-F9-C-0184 to the University of Illinois. The authors would like to thank H.H. Korst for his continued interest, encouragement, and support during the investigation.

References

- 1Addy, L., Korst, H.H., Walker, B.J., and White, R.A., "A Study of Flow Separation in the Base Region and its Effects during Powered Flight," AGARD-CP-124, April 1973.
- 2Alpinieri, L.J. and Adams, R.M., "Flow Separation due to Jet Pluming," *AIAA Journal*, Vol. 4, Oct. 1966, pp. 1865-1866.
- 3Deep, R.A., Henderson, J.H., and Brazzel, C.E., "Thrust Effects on Missile Aerodynamics," U.S. Army Missile Command, Redstone Arsenal, Ala., RD-TR-71-9, May 1971.
- 4Blackwell, K.L. and Hair, L.M., "Space Shuttle Afterbody Aerodynamics/Plume Simulation Data Summary," NASA TP 1384, 1978.
- 5Korst, H.H., White, R.A., Nyberg, S.-E., and Agrell, J., "Simulation and Modeling of Jet Plumes in Wind Tunnel Facilities," *Journal of Spacecraft and Rockets*, Vol. 18, Sept.-Oct. 1981, pp. 427-434.
- 6Korst, H.H., "Approximate Determination of Jet Contours near the Exit of Axially Symmetrical Nozzles as a Basis for Plume Modeling," U.S. Army Missile Command, Redstone Arsenal, Ala., TR-RD-72-14, Aug. 1972.
- 7Nyberg, S.-E., Agrell, J., and Hevren, T., "Investigation of Modeling Concepts for Plume-Afterbody Flow Interactions," 1st Annual Technical Report, Grant DA-ERO-78-G-028, The Aeronautical Research Institute of Sweden, Feb. 1979.
- 8Nyberg, S.-E. and Agrell, J., "Investigations of Modeling Concepts for Plume-Afterbody Flow Interactions," Final Technical Report, Grant DA-ERO-78-028, The Aeronautical Research Institute of Sweden, Nov. 1981.
- 9Nyberg, S.-E. and Agrell, J., "Effects of Control Fins and Angle of Attack on Plume Afterbody Flow Simulation," FFA, Annual Technical Report, Contract DAJA37-81-C-1213, The Aeronautical Research Institute of Sweden, Feb. 1983.
- 10Korst, H.H. and Deep, R.A., "Modeling of Plume Induced Interference Problems in Missile Aerodynamics," AIAA Paper 79-0362, Jan. 1979.
- 11Korst, H.H., Chow, W.L., and Zumwalt, G.W., "Research on Transonic Flow of a Real Fluid at Abrupt Increases in Cross Section (with Special Consideration of Base Drag Problems)—Final Report," University of Illinois, Urbana, Ill., Rept. ME-TN-392-5, Dec. 1959.
- 12Sims, J.L. and Blackwell, K.L., "Base Pressure Correlation Parameters," Missile and Plume Interaction Flow Fields Workshop, Redstone Arsenal, Ala., June 1977.
- 13Goethert, B.H. and Barnes, L.T., "Some Studies of the Flow Pattern at the Base of Missiles with Rocket Exhaust Jets," Arnold Engineering Development Center, Tullahoma, Tenn., AEDC-TR-58-12, June 1960.
- 14White, R.A., "Advanced Research/Analysis of Plume Induced Interference Flow," *Proceedings of the Symposium on "Rocket/Plume Fluid Dynamics Interactions"*, Huntsville, Ala., 1983.
- 15"FFA Wind Tunnel Facilities: Part 2—Transonic-Supersonic Tunnels," The Aeronautical Research Institute of Sweden (FFA), Bromman, Sweden, Memo. 93, 1969.
- 16White, R.A., Agrell, J., and Nyberg, S.-E., "The Wind Tunnel Simulation of Propulsive Jets and Their Modeling by Congruent Plumes Including Limits of Applicability," AIAA Paper 84-0232, Jan. 1984.